

## The development of geostrophic flow within a split cylinder

S.H. SMITH

*Department of Mathematics, University of Toronto, Toronto, M5S 1A1, Canada*

Received 9 March 1990; accepted in revised form 25 May 1990

**Abstract.** A description is given for the development of the flow inside connected rotating half-cylinders. Because there are no Ekman layers, spin-up does not occur, and so the time taken for the steady-state behaviour to be complete is  $O(E^{-1})$ ;  $E$  is the small Ekman number. However, a number of distinct stages in the process are recognized, and the interplay of the forces at each stage displayed. The main results are derived within a linear theory, but the adjustments required for a larger Rossby number are also described.

### 1. Introduction

The basic process in the development of flows in a rapidly rotating fluid is spin-up. Greenspan and Howard [1] showed in their fundamental paper how the fluid increases its angular velocity through vortex stretching in an  $O(E^{-1/2})$  time after an impulsive start, rather than the  $O(E^{-1})$  time expected if diffusion dominated;  $E$  is the small Ekman number. The theoretical prediction has been well verified experimentally (Benton and Clark [2]), and the essential role of the Ekman layer is well established – elements of fluid drawn into the layer from the interior spiral out, increasing their angular velocity throughout.

In their paper, Greenspan and Howard essentially concentrated on the simplest model where the flow is just between two parallel rotating plates. When an outer cylindrical boundary is included in the geometry a number of complications appear, and later work has tried to understand the behaviour as a wave front moves inward from the wall, with an angular velocity jump across the front; approximate analyses, numerical computations and experiments (Warn-Varnas, Fowles, Fiacek and Lee [3]) have combined to develop our understanding. The role of the Stewartson layer along the wall in this process has been less studied however, though recent work (Smith [4]) has described the development of such layers in a linear analysis of the split-disc model.

If there are no Ekman layers present, then it can be conjectured reasonably that the longer  $O(E^{-1})$  time will be required for the fluid to have its angular velocity increased after some impulsively induced change in the rotation speed of the boundary. The purpose of the present paper is to describe how the changes take place in the fluid. The model investigated is that of a split-cylinder; fluid rotates as a solid body inside an infinite circular cylinder when one half has its angular velocity increased, though only by an amount which ensures a small Rossby number. The steady-state behaviour for a fully linear flow was described some years ago by Hocking [5]. He showed how an almost inviscid geostrophic flow exists in the interior (the ratio of the radial to axial velocities is  $O(E)$ ), which is separated from the wall by a Stewartson layer. This work was continued by van Heijst [6], who gave a detailed analysis of the different shear layers along the wall of the cylinder when it has finite length. He showed that the matching of the interior flow to the sidewall is carried out partially by the  $\frac{1}{4}$ -layer, and partially by the  $\frac{1}{3}$ -layer, with the latter accounting for the jump discontinuity.

We confirm that the flow presented by Hocking requires the longer time; however, the Stewartson layer itself along the wall is formed by a process which is little changed from that described earlier for the split-disc geometry. At finite distances from the common rim, the almost geostrophic flow is effectively established in finite time, as the inviscid layer first described in [4] serves to focus all height-dependent change into the developing wall layer. The steady-state Stewartson layer is fully developed in the  $O(E^{-1/3})$  time; the axial velocity in the interior is unidirectional at this time with the mass flux balance maintained by a reverse flow in the layer. The final development of the circulation in the azimuthal plane described by Hocking does require the  $O(E^{-1})$  time as the velocities increase throughout this process.

These results are discussed within a linear theory, and we conclude by investigating the restrictions of such an approach. It is only when the Rossby number  $\varepsilon$  satisfies  $\varepsilon \ll E^{1/2}$  that the flow is everywhere linear; however, as long as  $\varepsilon \ll 1$  the inertial forces can be ignored outside the domain within  $O(\varepsilon)$  radial distances, and  $O(\varepsilon^3 E^{-1})$  axial distances from the rim between the cylinders. The nonlinear domain grows as the Rossby number increases.

## 2. The linear solution

We consider an infinite circular cylinder of radius  $a$ , filled with fluid of viscosity  $\nu$  and density  $\rho_0$ , which rotates with angular velocity  $\Omega$ . The cylinder has two sections. Without loss of generality, we investigate the symmetric situation where, at time  $t=0$ , the upper half is given an impulsive increase in angular velocity to  $\Omega(1+\varepsilon)$ , while the lower half is given an impulsive decrease to  $\Omega(1-\varepsilon)$ ; the constant  $\varepsilon$  represents the Rossby number for the motion, and we commence by taking  $\varepsilon$  to be sufficiently small so that all nonlinear terms can be neglected. We introduce a set of non-dimensional cylindrical co-ordinates  $(r, \theta, z)$ , where the cylinder is represented by  $r=1$ , and the split in the cylinder by  $z=0$ . The radial, azimuthal and axial velocities are written as  $\varepsilon\Omega au(r, z, t)$ ,  $\Omega a\{r + \varepsilon v(r, z, t)\}$  and  $\varepsilon\Omega aw(r, z, t)$  respectively, where  $a$  is the length scale and  $\Omega^{-1}$  the time scale. We can then write

$$u = -r^{-1}\psi_z, \quad v = r^{-1}\chi, \quad w = r^{-1}\psi_r, \quad (2.1)$$

to lead to the linear equations

$$2\chi_z = \left\{ E \left( \frac{\partial^2}{\partial r^2} - \frac{1}{r} \frac{\partial}{\partial r} + \frac{\partial^2}{\partial z^2} \right) - \frac{\partial}{\partial t} \right\} \left( \psi_r - \frac{1}{r} \psi_r + \psi_{zz} \right), \quad (2.2)$$

$$-2\psi_z = E \left( \chi_{rr} - \frac{1}{r} \chi_r + \chi_{zz} \right) - \chi_t; \quad (2.3)$$

$E = \nu/\Omega a^2$  is the Ekman number. The no-slip boundary conditions require

$$\psi = \psi_r = 0, \quad \chi = \text{sgn } z \quad \text{on } r = 1; \quad (2.4)$$

the initial condition is  $\psi = \chi = 0$  at  $t=0$ ,  $r \neq 1$ , and there is the additional requirement that  $\psi, \chi$  are bounded as  $z \rightarrow \pm\infty$ . Because of the symmetry introduced deliberately into the model, we can take  $z \geq 0$  in all which follows.

To solve these equations (2.2), (2.3), we define the Laplace transforms

$$\bar{\psi}(r, z, s) = \int_0^\infty e^{-st} \psi(r, z, t) dt, \quad \bar{\chi}(r, z, s) = \int_0^\infty e^{-st} \chi(r, z, t) dt,$$

and then take the Fourier transforms

$$\bar{\bar{\psi}}(r, \alpha, s) = \int_0^\infty \cos \alpha z \bar{\psi}(r, z, s) dz, \quad \bar{\bar{\chi}}(r, \alpha, s) = \int_0^\infty \sin \alpha z \bar{\chi}(r, z, s) dz.$$

These show the ordinary differential equations

$$\begin{aligned} 2\alpha \bar{\bar{\chi}} &= \left\{ E \left( \frac{\partial^2}{\partial r^2} - \frac{1}{r} \frac{\partial}{\partial r} - \alpha^2 \right) - s \right\} \left( \bar{\bar{\psi}}_{rr} - \frac{1}{r} \bar{\bar{\psi}}_r - \alpha^2 \bar{\bar{\psi}} \right), \\ 2\alpha \bar{\bar{\psi}} &= E \left( \bar{\bar{\chi}}_{rr} - \frac{1}{r} \bar{\bar{\chi}}_r - \alpha^2 \bar{\bar{\chi}} \right) - s \bar{\bar{\chi}}, \end{aligned} \quad (2.5)$$

together with the boundary conditions

$$\bar{\bar{\psi}} = \bar{\bar{\psi}}_r = 0, \quad \bar{\bar{\chi}} = (s\alpha)^{-1} \quad \text{on } r = 1. \quad (2.6)$$

The solution of (2.5) follows as

$$\bar{\bar{\chi}} = r \sum_{n=1}^3 A_n I_1(k_n r), \quad \bar{\bar{\psi}} = r \sum_{n=1}^3 B_n I_1(k_n r), \quad (2.7)$$

where  $I_1$  is the modified Bessel function; the constants  $k_n$  are the three roots with positive real part of the sixth-order equation

$$(k^2 - \alpha^2) \{ E(k^2 - \alpha^2) - s \}^2 = 4\alpha^2, \quad (2.8)$$

and the arbitrary constants  $A_n, B_n$  are connected by

$$2\alpha B_n = \{ E(k_n^2 - \alpha^2) - s \} A_n. \quad (2.9)$$

The boundary conditions (2.6) yield the three algebraic equations

$$\sum_{n=1}^3 A_n I_1(k_n) = (s\alpha)^{-1}, \quad \sum_{n=1}^3 B_n I_1(k_n) = 0, \quad \sum_{n=1}^3 B_n k_n I_1(k_n) = 0,$$

and these can be solved, using (2.9), in the form

$$\begin{aligned} \Delta B_1 &= (\pi E s \alpha^2)^{-1} \{ k_3 I_0(k_3) I_1(k_2) - k_2 I_0(k_2) I_1(k_3) \}, \\ \Delta B_2 &= (\pi E s \alpha^2)^{-1} \{ k_1 I_0(k_1) I_1(k_3) - k_3 I_0(k_3) I_1(k_1) \}, \\ \Delta B_3 &= (\pi E s \alpha^2)^{-1} \{ k_2 I_0(k_2) I_1(k_1) - k_1 I_0(k_1) I_1(k_2) \}, \end{aligned}$$

with

$$\Delta = \frac{k_1(k_3^2 - k_2^2)I_0(k_1)I_1(k_2)I_1(k_3)}{\{E(k_2^2 - \alpha^2) - s\}\{E(k_3^2 - \alpha^2) - s\}} + \frac{k_2(k_1^2 - k_3^2)I_0(k_2)I_1(k_1)I_1(k_3)}{\{E(k_1^2 - \alpha^2) - s\}\{E(k_3^2 - \alpha^2) - s\}} \\ + \frac{k_3(k_2^2 - k_1^2)I_0(k_3)I_1(k_1)I_1(k_2)}{\{E(k_1^2 - \alpha^2) - s\}\{E(k_2^2 - \alpha^2) - s\}}. \quad (2.10)$$

The formal solution for  $\bar{\psi}$ ,  $\bar{\chi}$  is now complete, and the inverse transforms give the final expressions for  $\psi$ ,  $\chi$ . Clearly the general formulae for  $\psi$ ,  $\chi$  require asymptotic or numerical evaluation for an interpretation of the physical behaviour, and these are now pursued for the different time domains of relevance.

The initial step is to analyze the algebraic equation (2.8) to determine the roots  $k_n$ . The major technical difference between the approach here and that of the earlier work of Smith [4] is that now we must solve for  $k$  in terms of  $\alpha$  because Fourier transforms in  $z$  have been taken, whereas previously  $\alpha$  was required in terms of  $k$  after Hankel transforms in  $r$  were taken. We are concerned with low Ekman number behaviour in rapidly rotating fluids; the relation between the two small parameters  $\varepsilon$ ,  $E$  for which these calculations will be valid is considered in Section 3.

(A) When  $t = O(1)$ , shear layers form along the cylinder wall, which begin to induce a circulation in the interior through the singularity at the rim. Mathematically, the roots for  $k$  from (2.8) show

$$k_1 \approx \alpha \left(1 + \frac{4}{s^2}\right)^{1/2}, \quad k_2, k_3 \approx \left(\frac{s}{E}\right)^{1/2} \quad \text{for } s = O(1); \quad (2.11)$$

the coefficients corresponding to this parameter domain can be found from (2.10) as

$$A_1 \approx -\frac{4E\alpha}{\pi s^4 I_1(k_1)}, \quad A_2, A_3 \approx \frac{\pi^{1/2}}{2^{1/2} E^{1/4} s^{3/4} \alpha} \exp\left\{-\left(\frac{s}{E}\right)^{1/2}\right\},$$

plus  $B_1 \approx -\frac{1}{2}s\alpha^{-1}A_1$ . The coefficients  $A_2$  and  $A_3$  give the contribution

$$\chi \approx \operatorname{erfc}\left(\frac{1-r}{2(Et)^{1/2}}\right) \quad \text{when } t = O(1), \quad (2.12)$$

as long as  $z \gg E^{1/2}$ , to represent the expected lateral diffusion in the shear layer which is developing along the wall. In the overlap region where both  $1-r$  and  $z$  are  $O(E^{1/2})$  diffusion in both the axial and radial directions must be included – this region is briefly investigated in (E).

Next, the coefficient  $B_1$  provides the dominant contribution to the stream function when  $t = O(1)$  away from the wall as

$$\psi \approx \frac{2Er}{\pi} \int_0^\infty \frac{I_1(\beta r)}{I_1(\beta)} d\beta \left\{ \frac{1}{2\pi i} \int_{c-i\infty}^{c+i\infty} \frac{e^{s't}}{s(s^2+4)^{1/2}} \cos\left(\frac{\beta sz}{(s^2+4)^{1/2}}\right) ds \right\}, \quad (2.13)$$

which displays the development of the circulation within the interior; the radial and axial velocities are  $O(E)$  in magnitude. For small times  $t$  an approximation to (2.13) shows

$$\psi \approx \frac{Ert^2}{\pi} \int_0^\infty \frac{I_1(\beta r)}{I_1(\beta)} \cos \beta z \, d\beta \quad \text{for } z, 1-r = O(1);$$

this function  $\psi$  satisfies  $L_{-1}\psi = 0$ , and represents a ring dipole at  $z = 0, r = 1$ . We do not write  $\psi$  as a sum of higher-order multipoles here, as can be obtained from (2.13) on taking the inverse Laplace transform, but note that for large  $t$  a separate approximation shows

$$\psi \approx \frac{Ert}{\pi} \int_0^\infty \frac{I_1(\beta r)}{I_1(\beta)} \, d\beta \quad \text{for } t \gg 1, \quad z = O(1). \tag{2.14}$$

Already the stream function is independent of  $z$  and so the radial velocity is zero to this order in the interior, while the axial velocity is given by

$$w \approx \frac{Et}{\pi} \int_0^\infty \frac{\beta I_0(\beta r)}{I_1(\beta)} \, d\beta \quad \text{for } t \gg 1, \quad z = O(1). \tag{2.15}$$

The graph of (2.15) is given in Fig. 1; there is singular behaviour as  $r \rightarrow 1-$ , with the limiting form  $w \approx E\pi^{-1}t(1-r)^{-2}$ . The geostrophy with a purely axial flow in the interior is established as  $t$  increases through  $O(1)$  values at finite distances from the junction; the circulation pattern in the interior has decayed. The axial velocity (2.15) is positive for all  $r$ , and it follows that there must be a negative axial velocity in the developing layer along the cylinder wall to preserve the mass flux balance. Similarly, we can form the integral for  $\chi$  corresponding to (2.14) using the coefficient  $A_1$ , and see that the azimuthal velocity  $v$  is given by

$$v \approx -\frac{Ez}{2\pi} \int_0^\infty \frac{\beta^2 I_1(\beta r)}{I_1(\beta)} \, d\beta \quad \text{for } t \gg 1, \quad z = O(1); \tag{2.16}$$

the graph of (2.16) is given in Fig. 2.

A particular computation from (2.13) which can be completed is that on the mid-plane, where it is seen that

$$w(r, 0, t) = \frac{2E}{\pi} \int_0^\infty \frac{\beta I_0(\beta r)}{I_1(\beta)} \, d\beta \mathcal{W}(t) \quad \text{for } t = O(1),$$

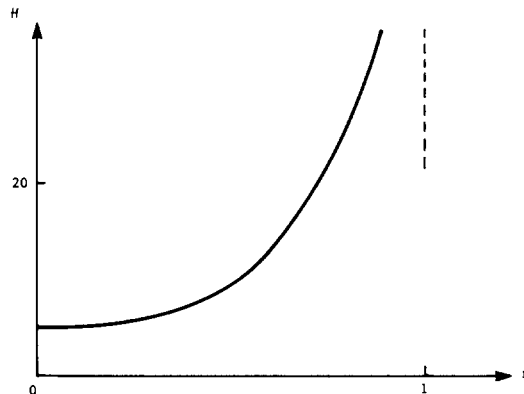


Fig. 1. The axial velocity in the interior;  $w = E\pi^{-1}t\mathcal{H}(r)$  from (2.15).

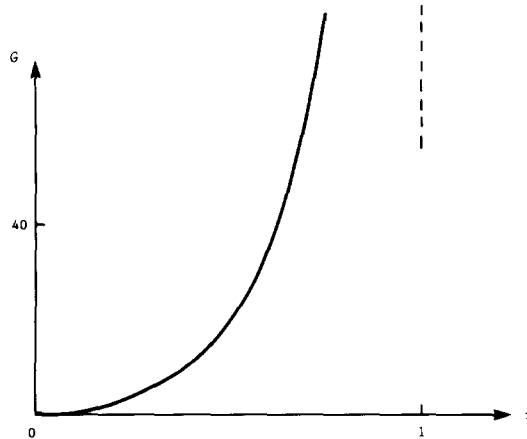


Fig. 2. The azimuthal velocity in the interior;  $v = -\frac{1}{2}E\pi^{-1}z\mathcal{G}(r)$  from (2.16).

where

$$\mathcal{W}(t) = \mathcal{L}^{-1}\{s^{-2}(s^2 + 4)^{-1/2}\} = \frac{1}{2}t \left[ \int_0^{2t} J_0(u) du - J_1(2t) \right]; \tag{2.17}$$

the graph of  $\mathcal{W}(t)$  is given in Fig. 3, which shows how the oscillation about the mean flow decays as  $t$  increases.

For large  $t$ , it can be observed from the integral (2.13) that  $\psi$  can be written as  $\psi \approx Etf(r, zt^{-1})$  for some function  $f$ , and so the circulation with  $O(Et)$  velocities is still present far from the junction in the domain where  $zt^{-1} = O(1)$ .

(B) We now see that the singular behaviour for  $w$  and  $v$  as  $r \rightarrow 1-$  in the core is a consequence of the development of the inviscid layer along the wall as  $t$  increases. The result follows from extending the approximation given in (2.11) for the roots of (2.8) to show

$$k_1 \approx \frac{2\alpha}{s}, \quad k_2 \approx \left(\frac{s}{E}\right)^{1/2} + \frac{\alpha}{s}, \quad k_3 \approx \left(\frac{s}{E}\right)^{1/2} - \frac{\alpha}{s}, \quad s \ll 1, \tag{2.18}$$

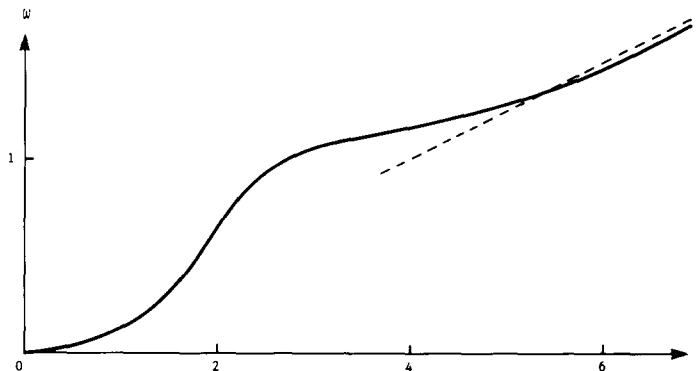


Fig. 3. The development of the geostrophic axial velocity in time;  $\mathcal{W}(t)$  is defined in (2.17).

from which we find

$$B_1 \approx \frac{4E\alpha^{1/2}}{\pi^{1/2}s^{7/2}} \exp\left\{-\frac{2\alpha}{s}\right\}, \quad B_2 \approx \frac{2^{1/2}E^{1/4}}{\pi^{1/2}s^{5/4}\alpha} \exp\left\{-\left(\frac{s}{E}\right)^{1/2} - \frac{\alpha}{s}\right\},$$

$$B_3 \approx -\frac{2^{1/2}E^{1/4}}{\pi^{1/2}s^{5/4}\alpha} \exp\left\{-\left(\frac{s}{E}\right)^{1/2} + \frac{\alpha}{s}\right\}, \quad \text{plus } A_1 \approx \frac{2\alpha}{s} B_1.$$

The contribution from the root  $k_1$  shows that

$$\psi \approx \frac{Et}{\pi(1-r)} \left\{1 - \frac{\sin \lambda}{\lambda}\right\}, \quad \chi \approx \frac{Et}{\pi(1-r)^2} \left\{\sin \lambda - \frac{2}{\lambda}(1 - \cos \lambda)\right\}, \quad (2.19)$$

in the domain  $\lambda = O(1)$ , where we have written

$$\lambda = \frac{2(1-r)t}{z}.$$

The similarity variable  $\lambda$  defines a layer along the wall where there is a time dependent geostrophic balance between the inviscid terms  $2\chi_z = -\psi_{rr}$ ,  $2\psi_z = \chi_t$ , the graphs of the velocities given by (2.19) are given in Fig. 4.

When we take the limit  $\lambda \rightarrow \infty$  in (2.19), we see that  $\psi \approx E\pi^{-1}t(1-r)^{-1}$ , which matches with the limit of (2.14) as  $r \rightarrow 1^-$ . This flow in the layer develops as  $t$  increases, and separates the increasing axial flow in the interior from the viscous shear layer along the cylinder wall; it is the shear layer which ensures the no-slip conditions are satisfied on the surface of the wall. The limit of (2.19) as  $\lambda \rightarrow 0$  shows  $\psi \approx \frac{2}{3}E\pi^{-1}t^3z^{-2}(1-r)$ , which indicates the slip velocity  $-\frac{2}{3}E\pi^{-1}t^3z^{-2}$  along the wall from inviscid theory. The stream function in this shear layer follows from the contribution given by the roots  $k_2, k_3$ ; specifically,

$$\psi \approx -\frac{Et^3}{180\pi z^2} \left[ 120 - (\rho^6 + 30\rho^4 + 180\rho^2 + 120) \operatorname{erfc}\left(\frac{1}{2}\rho\right) \right]$$

$$+ 2\pi^{-1/2}\rho(\rho^4 + 28\rho^2 + 132)e^{-1/4\rho^2},$$

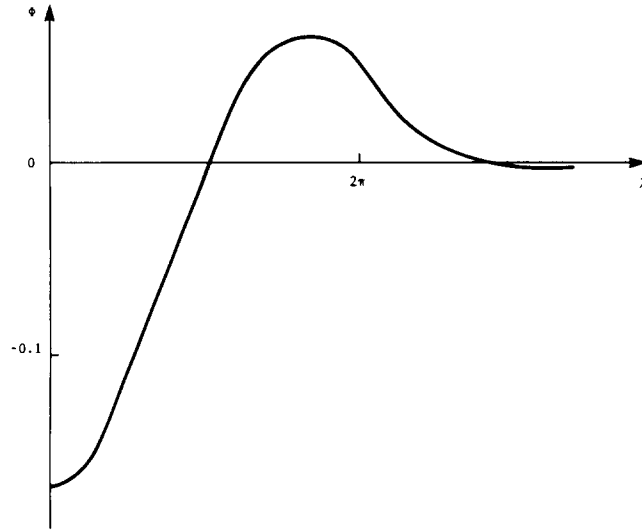
where  $\rho = (1-r)/(Et)^{1/2}$ .

Finally we note that the inviscid geostrophic region has width  $O(z/t)$  when  $\lambda = O(1)$ , and so it overlaps with the shear layer where  $\rho = O(1)$  in the domain where  $1-r = O\{(Et)^{1/2}\}$ ,  $z = O(E^{1/2}t^{3/2})$ ; here both effects are present.

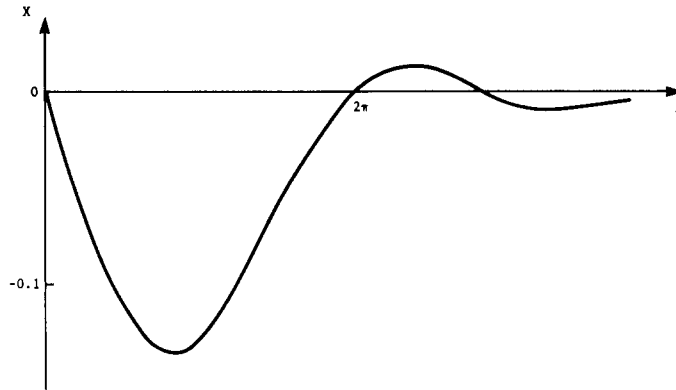
(C) Next, we observe that for  $z = O(1)$  the two layers where  $1-r = O(E^{1/2}t^{1/2})$  and  $O(z/t)$  coalesce when  $t = O(E^{-1/3})$  to give a single domain with  $1-r = O(E^{1/3})$  – the Stewartson layer. More precisely, at general height  $z$ , we have a domain defined by  $\mu = O(1)$  where

$$\mu = \frac{1-r}{(Ez)^{1/3}}, \quad (2.20)$$

which is consolidated when  $t = O(E^{-1/3}z^{-1/3})$ ; this domain is formed through the growth of the overlap region described at the end of the previous subsection.



(a)



(b)

Fig. 4. The velocities in the shear layer during the inviscid stage; (a)  $\psi_r = (4Et^3/\pi z^2)\Phi(\lambda)$  and (b)  $\chi = (4Et^3/\pi z^2)X(\lambda)$  from (2.19).

The form of the algebraic equation (2.8) required for the description of the behaviour within this region where  $\mu = O(1)$  is approximately

$$\kappa^3 - q\kappa \pm 2\alpha = 0, \tag{2.21}$$

where  $k = E^{-1/3}\kappa$ ,  $s = E^{1/3}q$  and  $\kappa, q, \alpha = O(1)$ ; only the three roots  $\kappa_i$  with positive real part from (2.21) are included. Completing the details shows

$$\kappa_1 = (\gamma + \alpha)^{1/3} - (\gamma - \alpha)^{1/3}, \quad \kappa_2 = -\omega(\gamma + \alpha)^{1/3} + \omega^2(\gamma - \alpha)^{1/3}, \tag{2.22}$$

$$\kappa_3 = -\omega^2(\gamma + \alpha)^{1/3} + \omega(\gamma - \alpha)^{1/3}, \quad \text{for } \gamma = (\alpha^2 - q^3/27)^{1/2}; \quad \text{here } \omega = e^{2\pi i/3}.$$



Hence

$$\psi \approx \frac{E^{1/3}}{2\pi^2 i} \int_{c-i\infty}^{c+i\infty} \frac{e^{qr}}{q} dq \int_0^\infty \frac{\cos \alpha z}{\alpha \kappa_1^2} \left\{ \kappa_1 e^{-\kappa_1 \sigma} + \frac{i\kappa_2}{\sqrt{3}} e^{-\kappa_2 \sigma} - \frac{i\kappa_3}{\sqrt{3}} e^{-\kappa_3 \sigma} \right\} d\alpha.$$

for  $1-r = E^{1/3}\sigma$ ,  $t = E^{-1/3}\tau$ , with a similar expression for  $\chi$ . As  $\tau \rightarrow 0$ , the result (2.19) follows. As  $\tau \rightarrow \infty$ , a steady state is reached within the layer; the roots  $\kappa_i$  for  $q \rightarrow 0$  show  $\kappa_1 \approx (2\alpha)^{1/3}$ ,  $\kappa_2 \approx e^{-i\pi/3}\kappa_1$ ,  $\kappa_3 \approx e^{i\pi/3}\kappa_1$  and so

$$\begin{aligned} \psi &\approx (Ez)^{1/3} \phi(\mu) = \frac{(Ez)^{1/3}}{2^{1/3}\pi} \int_0^\infty \frac{\cos u}{u^{4/3}} \left\{ e^{-(2u)^{1/3}\mu} - e^{-1/2(2u)^{1/3}\mu} \cos \frac{\sqrt{3}}{2} (2u)^{1/3}\mu \right. \\ &\quad \left. + \frac{1}{\sqrt{3}} e^{-1/2(2u)^{1/3}\mu} \sin \frac{\sqrt{3}}{2} (2u)^{1/3}\mu \right\} du, \\ \chi &\approx \frac{1}{\pi} \int_0^\infty \frac{\sin u}{u} \left\{ e^{-(2u)^{1/3}\mu} + e^{-1/2(2u)^{1/3}\mu} \cos \frac{\sqrt{3}}{2} (2u)^{1/3}\mu \right. \\ &\quad \left. + \frac{1}{\sqrt{3}} e^{-1/2(2u)^{1/3}\mu} \sin \frac{\sqrt{3}}{2} (2u)^{1/3}\mu \right\} du \end{aligned}$$

for  $\tau \rightarrow \infty$ ; the graphs of these functions are given in Fig. 5. The Stewartson  $\frac{1}{3}$ -layer is formed in the limit as  $\tau \rightarrow \infty$ ; although Hocking [5] did not write down these expressions, they can be gained directly from his results after taking asymptotic approximations. In particular,  $\phi'(\mu) \rightarrow 1/\sqrt{3}$  as  $\mu \rightarrow \infty$ , which shows the axial velocity  $-\varepsilon\Omega a/\sqrt{3}$  at the edge of the boundary layer.

The Stewartson layer is fully formed when  $t = O(E^{-1/3})$  for  $z = O(1)$ ; however, for large  $z$  it requires the extended time  $t = O(E^{-1/3}z^{2/3})$  for the steady state to be achieved.

(D) Within the interior the axial velocity given by (2.15), developed during finite time, is valid for all  $t \ll E^{-1}$  when  $z = O(1)$ , and the reversed flow is still within the wall layer. This

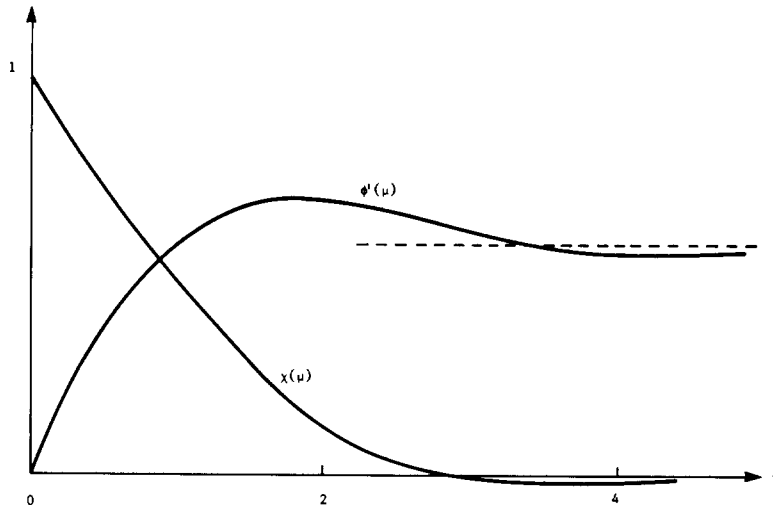


Fig. 5. The velocities in the steady state Stewartson layer;  $w \approx -\phi'(\mu)$  and  $v \approx \chi(\mu)$  from (2.23).

layer has width  $O(E^{1/3})$  when  $t = O(E^{-1/3})$ , but for  $E^{-1/3} \ll t \ll E^{-1}$  diffusion still acts as the layer with width  $O(E^{1/2}t^{1/2})$  continues to widen. The final steady state in the interior described by Hocking does require the  $O(E^{-1})$  time before it is fully developed.

To describe the behaviour here we write (2.8) as

$$k^3 - pk \pm 2\beta = 0, \quad (2.23)$$

with  $s = Ep$ ,  $\alpha = E\beta$ , for  $k, p, \beta = O(1)$ ; the equation (2.23) is equivalent to (2.21), and so the roots  $k_i$  ( $i = 1, 2, 3$ ) can be written down directly from (2.22). The representation for the stream function is

$$\begin{aligned} \psi \approx & \frac{2r}{\pi^3 i} \int_{c-i\infty}^{c+i\infty} \frac{e^{pEt}}{p} dp \int_0^\infty \frac{\cos \beta Ez}{\tilde{\Delta}\beta} [\{k_3 I_0(k_3) I_1(k_2) - k_2 I_0(k_2) I_1(k_3)\} I_1(k_1 r) \\ & + \{k_1 I_0(k_1) I_1(k_3) - k_3 I_0(k_3) I_1(k_1)\} I_1(k_2 r) \\ & + \{k_2 I_0(k_2) I_1(k_1) - k_1 I_0(k_1) I_1(k_2)\} I_3(k_3 r)] d\beta, \end{aligned}$$

where

$$\begin{aligned} \tilde{\Delta} = & (k_3^2 - k_2^2) I_0(k_1) I_1(k_2) I_1(k_3) + (k_1^2 - k_3^2) I_0(k_2) I_1(k_2) I_1(k_3) \\ & + (k_2^2 - k_1^2) I_0(k_3) I_1(k_2) I_1(k_1), \end{aligned}$$

with a corresponding form for  $\chi$ .

Besides taking the limit  $Et \rightarrow \infty$  to regain Hocking's solution, the only worthwhile approximation which can be gained from this expression is in the domain where  $\rho, \zeta = O(1)$ , with

$$\rho = \frac{1-r}{(Et)^{1/2}}, \quad \zeta = \frac{z}{E^{1/2}t^{3/2}}.$$

Here we can write

$$\psi \approx \frac{(Et)^{1/2}}{2\pi^2 i} \int_{c-i\infty}^{c+i\infty} \frac{e^u}{u} du \int_0^\infty \frac{\cos v\zeta}{\delta_1^2 v} \left[ \delta_1 e^{-\delta_1 \rho} + \frac{i}{\sqrt{3}} \delta_2 e^{-\delta_2 \rho} - \frac{i}{\sqrt{3}} \delta_3 e^{-\delta_3 \rho} \right] dv,$$

where  $\delta_i$  are the roots with positive real part of  $\delta^3 - \delta \pm 2v = 0$ , numbered as was done with (2.21). When  $z = O(1)$ , and so  $\zeta = 0$ , for the limit  $\rho \rightarrow 0$  we see that  $\psi_\rho \approx -3^{-1/2}$  to match with the axial velocity at the edge of the steady  $\frac{1}{3}$ -layer, and when  $\rho \rightarrow \infty$ ,  $\psi_\rho \approx \pi^{-1} \rho^{-2}$  to match with the axial velocity at the edge of the interior region as given in (2.15). Consequently, the value of  $r$  at which the axial velocity is zero (for finite  $z$ ) moves into the body of fluid within this diffusion layer where  $1-r = O(E^{1/2}t^{1/2})$ . Eventually, as  $t$  becomes  $O(E^{-1})$ , the position where flow reversal takes place moves into the interior region, finally settling at  $r \approx 0.6$  according to Hockings computations.

(E) So far we have ignored the innermost region where both  $1-r$  and  $z$  are  $O(E^{1/2})$ . To fully describe the flow here requires taking both  $\alpha$  and  $k$  to be  $O(E^{-1/2})$ , with  $s = O(1)$ , in the equation (2.8); consequently, no simplification is possible in the expression for the roots,

nor worthwhile expressions for the velocities. The only general result is that all the transient behaviour does take place during finite time  $t$ . However, if we write  $1 - r = E^{1/2}\mathcal{X}$ ,  $z = E^{1/2}\mathcal{Y}$ , and proceed to take  $\mathcal{X}$  and  $\mathcal{Y}$  themselves to be small, some understanding of the flow close to the singularity at  $r = 1$ ,  $z = 0$  is gained.

Here the left hand side of (2.3) is negligible to give the simplified equation  $\chi_{\mathcal{X}\mathcal{X}} + \chi_{\mathcal{Y}\mathcal{Y}} = \chi_t$ , with  $\chi = \text{sgn } \mathcal{Y}$  on  $\mathcal{X} = 0$ ; including the initial condition then leads to

$$\bar{\chi} = \frac{2}{\pi s} \int_0^\infty \frac{\sin \beta \mathcal{Y}}{\beta} e^{-(\beta^2+s)^{1/2}\mathcal{Y}} d\beta, \quad \mathcal{X}, \mathcal{Y} \ll 1. \quad (2.24)$$

(This can of course be obtained from the general solution, but the complications involved are unnecessary.) Now (2.24) described the strictly two-dimensional flow due to the two halves of a split-plane moving in opposite directions with diffusion alone acting; as  $t \rightarrow \infty$ ,  $\chi \approx 2\omega/\pi$ , where  $\mathcal{X} = \mathcal{R} \cos \omega$ ,  $\mathcal{Y} = \mathcal{R} \sin \omega$ , as given by van Heijst [6].

The stream function now follows from (2.2), which can be solved to give

$$\bar{\psi} = \frac{2E^{1/2}}{\pi s^3(\beta^2+s)^{1/2}} \left[ \{(\beta^2+s)^{1/2} + \beta\} \{e^{-\beta\mathcal{X}} - e^{-(\beta^2+s)^{1/2}\mathcal{X}}\} - s\mathcal{X} e^{-(\beta^2+s)^{1/2}\mathcal{X}} \right]$$

for  $\beta = E^{1/2}\alpha$  in the Fourier transform. The velocity is finite for all  $\mathcal{X}$ ,  $\mathcal{Y} = O(1)$ , with the dominant contribution being in the axial direction as  $t \rightarrow \infty$ , with magnitude  $(2\pi)^{-1}E^{1/2}\mathcal{R}^2 \ln \mathcal{R} \cos^2\theta$  for  $\mathcal{R} \ll 1$ . The other result to note is that the stress on the wall of the cylinder near the singularity is

$$2\pi^{-1}\rho_0\nu E^{1/2}t^{1/2} \int_0^\infty \cos(\gamma\mathcal{Y}t^{-1/2}) \left\{ \text{erfc } \gamma + \frac{1}{2} \gamma^{-2} \text{erf } \gamma - \pi^{-1/2}\gamma^{-1} e^{-\gamma^2} \right\} d\gamma,$$

( $\rho_0$  is the density) which is bounded at all times, and gives  $4\pi^{-3/2}\rho_0\nu E^{1/2}t^{1/2}$  as  $\mathcal{Y}t^{-1/2} \rightarrow 0$ .

We complete this section with two final observations. Firstly, the infinite geometry in the axial direction permits a scaling of the variables to eliminate the Ekman number  $E$  from the dominant terms of the basic equations (2.2), (2.3) and consequently, because the boundary conditions are independent of  $E$ , from the linear problem as a whole; Hocking [5] noted this for the steady state case. We write

$$r = R, \quad z = E^{-1}Z, \quad t = E^{-1}T,$$

for

$$2\chi_Z = \left( \frac{\partial^2}{\partial R^2} - \frac{1}{R} \frac{\partial}{\partial R} - \frac{\partial}{\partial T} \right) (\psi_{RR} - \frac{1}{R} \psi_R), \quad -2\psi_Z = \chi_{RR} - \frac{1}{R} \chi_R - \chi_T.$$

Because there is no Ekman layer the  $\partial^2/\partial z^2$  terms in (2.2), (2.3) play no role in the development of the motion.

Also, if the geometric model is changed slightly to the collar  $|z| < c$  (for some constant  $c$ ) of the cylinder having its angular velocity increased from  $\Omega$  to  $\Omega(1 + \varepsilon)$  time  $t = 0$ , it can be seen that the functions  $\psi_c(r, z, t)$  for the motion will be given by

$$\begin{aligned} \psi_c(r, z, t) &= \psi_0(r, z + c, t) - \psi_0(r, z - c, t), \\ \chi_c(r, z, t) &= \chi_0(r, z + c, t) - \chi_0(r, z - c, t), \end{aligned}$$

where  $\psi_0$  and  $\chi_0$  are the corresponding functions already found for the single split at  $z = 0$  for all the separate time domains. The function  $\psi_c$  is now an odd function of  $z$ , as  $\psi_0$  is even; the reverse is true for  $\chi$ . Therefore, there will be no interior flow to leading order once  $t \gg 1$ , and from then on it is only in the wall layer that the effect of the differential rotation is noticed.

### 3. The nonlinear correction

So far the nonlinear terms have been completely ignored on the basis that the Rossby number  $\varepsilon$  is sufficiently small. However, because there is a discontinuity in the azimuthal velocity on the boundary  $r = 1$  at  $z = 0$ , it is necessary to consider the existence of a region in the neighbourhood of the junction of the cylinders where the velocity gradients are large enough that inertial terms must be included in the basic balance of forces.

When  $\Omega a U$ ,  $\Omega a V$ ,  $\Omega a W$  are the radial, azimuthal and axial velocities respectively in the fluid,  $\rho_0 \Omega^2 a^2 P$  is the pressure, then the complete Navier–Stokes equations are

$$U_r + r^{-1}U + W_z = 0, \quad (3.1)$$

$$U_t + UU_r + WU_z - r^{-1}V^2 = -P_r + E(U_{rr} + r^{-1}U_r - r^{-2}U + U_{zz}), \quad (3.2)$$

$$V_t + UV_r + r^{-1}UV + WV_z = E(V_{rr} + r^{-1}V_r - r^{-2}V + V_{zz}), \quad (3.3)$$

$$W_t + UW_r + WW_z = -P_z + E(W_{rr} + r^{-1}W_r + W_{zz}); \quad (3.4)$$

the approximation in Section 2 was to write  $U = \varepsilon u$ ,  $V = r + \varepsilon v$ ,  $W = \varepsilon w$ ,  $P = \frac{1}{2}r^2 + \varepsilon p$ , and then neglect all quadratic terms in  $\varepsilon$ .

To begin, we observe that the inertial terms are required in the innermost domain where  $1 - r$ ,  $z = O(E^{1/2})$  once the Rossby number is large enough that  $\varepsilon = O(E^{1/2})$ . This is the minimum value of  $\varepsilon$  for which the linear theory breaks down, and the full equations need to be considered here for all times  $t$ , though for no times outside this domain. We proceed to take  $\varepsilon \gg E^{1/2}$  in all which follows.

We now consider the formation of the geostrophic layer in which  $\lambda = 2(1 - r)t/z = O(1)$ . From (2.19) it is clear that the azimuthal velocity shows  $V_r = 1 + O\{\varepsilon Et(1 - r)^{-3}\}$ , and so the nonlinear terms are necessary when

$$1 - r = O(\varepsilon^{1/3} E^{1/3} t^{1/3}), \quad z = O(\varepsilon^{1/3} E^{1/3} t^{4/3}). \quad (3.5)$$

Here  $V$  and  $W$  are  $O(\varepsilon^{1/3} E^{1/3} t^{1/3})$ , and the basic momentum balance requires the inertial forces in the azimuthal and axial directions (i.e. equations (3.3) and (3.4)); the viscous terms are still negligible. It is the focusing of the action into the narrow region defined by the similarity variable  $\lambda$  which increases the velocities, and so leads to the nonlinearity, which begins to develop as  $t$  increases through finite values. Although the velocities will be given in terms of  $\lambda$  (by (2.19)) at the outer edge of the domain (3.5), within it such a simple representation is no longer possible. This domain is larger than the overlap region between the geostrophic and diffusion layers (where  $1 - r = O(E^{1/2} t^{1/2})$ ,  $z = O(E^{1/2} t^{3/2})$ ) only as long as  $t \ll \varepsilon^2 E^{-1}$ , and so a separate analysis is necessary when this time constraint is no longer satisfied.

For  $t = O(\varepsilon^2 E^{-1})$ , both regions have the common width  $O(\varepsilon)$  and height  $O(\varepsilon^3 E^{-1})$ , and we write

$$1 - r = \varepsilon \eta, \quad z = \varepsilon^3 E^{-1} \xi, \quad t = \varepsilon^2 E^{-1} \theta \quad (3.6)$$

with the velocities given by

$$U = E \varepsilon^{-1} F, \quad V = r + \varepsilon G, \quad W = \varepsilon H, \quad P = \frac{1}{2} r^2 + \varepsilon^2 S,$$

to give the equations

$$\begin{aligned} -F_\eta + H_\xi &= 0, & 2G &= -S_\eta, \\ G_\theta - FG_\eta + HG_\xi &= G_{\eta\eta}, & H_\theta - FH_\eta + HH_\xi &= -P_\xi + H_{\eta\eta}; \end{aligned} \quad (3.7)$$

the viscous forces are now included along with the inertial forces. It is noted that the similarity variable  $\mu$  for the Stewartson  $\frac{1}{3}$ -layer satisfies  $\mu = O(1)$  in this domain  $\eta, \xi = O(1)$ . As long as  $\varepsilon$  is small, the extent of the nonlinearity is therefore restricted to this domain, and it is as  $\theta \rightarrow \infty$  that the steady state is fully developed here. Outside  $\eta, \xi = O(1)$  the motion is correctly given by the linear behaviour described in Section 2 for all times.

Now the steady state form of the equations (3.7) are equivalent to those discussed by Stewartson [7], when he was considering the formation of boundary layers induced by the axial pressure gradient along the surface of a rotating circular cylinder; in Stewartson's work the Rossby number is finite, and the one change from (3.7) is that the centrifugal term is also nonlinear in the angular momentum equation. His discussion can be adapted directly to the present situation; here we can define a similarity variable  $\phi = \eta \xi^{-2/5}$  for a wall layer where the no-slip conditions need be satisfied, and then develop a series solution (with, for example,  $G = \sum_{n=0}^{\infty} \xi^{2n/5} G_n(\phi)$ ) leading to a set of ordinary differential equations for  $G_n$ , etc., which can be solved iteratively. However, when the numerical solution of the differential equations for the leading-order terms are investigated it is found that one exists only for  $\xi < 0$ . The symmetry about  $z = 0$ , present throughout the linear solution, is lost within this nonlinear region. The nature of the behaviour here is somewhat complex even for the steady-state situation, and we just sketch the details. When  $z < 0$  there is, in fact, a double structure: the inner viscous region where  $\phi = O(1)$  has the viscous terms present to leading order, but the Coriolis term absent, and the outer inertial region where the Coriolis term is present to leading order, but the viscous terms are absent. The situation is roughly similar to, but necessarily more detailed than, the flow near the trailing edge of a flat plate (c.f. Goldstein [8]).

The development of the inner region in time is through diffusion as the axial velocity induced by the differential rotation grows, with  $1 - r = O(E^{1/2} t^{1/2})$ ; it extends down the wall as  $|z| = O(\varepsilon^{1/2} E^{1/4} t^{5/4})$ . Because  $\varepsilon^{1/2} E^{1/4} t^{5/4} \gg \varepsilon^{1/3} E^{1/3} t^{4/3}$  for  $t \ll \varepsilon^2 E^{-1}$  (n.b. (3.5)), it follows that this growth of nonlinearity along the wall is a distinct process from that described earlier, which is an inviscid process. However, both processes coincide once  $t = O(\varepsilon^2 E^{-1})$  as the final nonlinear domain (3.6) is consolidated.

The author wishes to thank the Natural Sciences and Engineering Research Council of Canada for a research grant during the time this work was completed.

## References

1. H.P. Greenspan and L.M. Howard, On a time dependent motion of a rotating fluid, *J. Fluid Mech.* 17 (1963) 385–404.
2. E.R. Benton and A. Clark, Jr., Spin-up, *Ann. Rev. Fluid Mech.* 6 (1974) 257–280.
3. A. Warn-Varnas, W.W. Fowles, S. Piacsek and S.M. Lee, Numerical solutions and laser-Doppler measurements of spin-up, *J. Fluid Mech.* 85 (1978) 609–639.
4. S.H. Smith, The formation of Stewartson layers in a rotating fluid, *Quart. J. Mech. appl. Math.* (1987) 575–594.
5. L.M. Hocking, An almost-inviscid geostrophic flow, *J. Fluid Mech.* 12 (1962) 129–134.
6. G.J.F. van Heijst, The shear layer structure in a rotating fluid near a differentially rotating sidewall, *J. Fluid Mech.* 130 (1983) 1–12.
7. K. Stewartson, On rotating laminar boundary layers, *Boundary Layer Research Symposium* (1958) 59–71 (Springer, Berlin).
8. S. Goldstein, Concerning some solutions of the boundary layer equations in hydrodynamics, *Proc. Camb. Phil. Soc.* 26 (1930) 1–30.